JACS
JOURNAL OF THE AMERICAN CHEMICAL SOCIETY
pubs.acs.org/JACS
Article

^{14}N to ^{15}N Isotopic Exchange of Nitrogen Heteroaromatics through Skeletal Editing

G. Logan Bartholomew, Samantha L. Kraus, Lucas J. Karas, Filippo Carpaneto, Raffeal Bennett, Matthew S. Sigman,* Charles S. Yeung,* and Richmond Sarpong*

Cite This: J. Am. Chem. Soc. 2024, 146, 2950−2958

Read Online

ACCESS | Metrics & More | Article Recommendations | Supporting Information

ABSTRACT: The selective modification of nitrogen heteroaromatics enables the development of new chemical tools and accelerates drug discovery. While methods that focus on expanding or contracting the skeletal structures of heteroaromatics are emerging, methods for the direct exchange of single core atoms remain limited. Here, we present a method for $^{14}N \rightarrow {}^{15}N$ isotopic exchange for several aromatic nitrogen heterocycles. This nitrogen isotope transmutation occurs through activation of the heteroaromatic substrate by triflylation of a nitrogen atom, followed by a ring-opening/ring-closure sequence mediated by ^{15}N-aspartate to effect the isotopic exchange of the nitrogen atom. Key to the success of this transformation is the formation of an isolable ^{15}N-succinyl intermediate, which undergoes elimination to give the isotopically labeled heterocycle. These transformations occur under mild conditions in high chemical and isotopic yields.

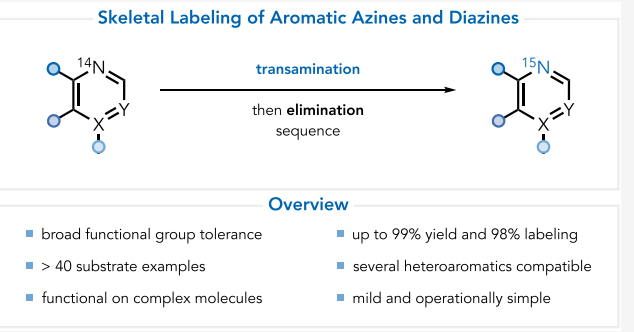

INTRODUCTION

The incorporation of traceable isotopes into organic molecules has diverse applications across chemistry, biology, and materials science. Specifically, isotopic labeling is instrumental in studying organic reaction mechanisms and evaluating biologically relevant molecules.[1,2] Nitrogen-15 labeling, in particular, induces dipolar NMR activity in nitrogen-containing compounds, thus enabling the utilization of various powerful analytical techniques (Figure 1A).[1,3−5] Nitrogen heterocycles are prevalent in drug compounds, agrochemicals, materials, and natural products, making their selective modification crucial for discovery campaigns in these industries.[6−8] Given the ubiquity of nitrogen heterocycles in functional molecules, especially pharmaceuticals, and the significance of isotopic labeling in applications like biomolecular NMR,[1,3−5] structural analysis,[9] *in vivo* metabolomics,[10−12] mechanism elucidation, solution-state mechanics,[13−18] and spin hyperpolarization (particularly by SABRE-SHEATH, Figure 1B),[19−21] we anticipated that a direct method for isotopically labeling nitrogen heteroaromatics would be highly valuable. Though Chekmenev et al. reported an isotope exchange of nicotinamide[22] using established Zincke[23,24] transamination in 2016, this methodology requires harsh conditions for activation and ring closure, severely limiting substrate scope. Even modest levels of isotopic labeling (8−10% ^{15}N) can considerably enhance signal-to-noise ratios in ^{15}N NMR, enabling such commonly used techniques in the analysis of isotopically impure compounds.[25−27]

Nonetheless, applications of ^{15}N-labeled compounds are limited by the availability of enriched reagents to prepare labeled compounds through chemical means,[18] with ^{15}N-labeled amino acids being the most common reagents. Existing methods for isotopic labeling of heteroaromatic nitrogen(s) are generally inefficient, often necessitating the *de novo* synthesis of the desired enriched isotopologues or harsh conditions for Zincke transamination.[14,18,28−30] Therefore, an approach to directly label the skeletons of such compounds would be of great value.

To achieve this goal, we envisioned a skeletal editing tool. The field of skeletal editing has been rapidly expanding,[31] although most studies focus on altering skeletal frameworks (Figure 1C). Methods for the direct exchange of atoms constituting the core of nitrogen heterocycles without changing their structural topography (i.e., atom transmutation) remain scarce, although reports toward this goal are emerging (Figure 1D,E). In 2022, Patel and Burns reported a sequential nitrogen insertion/carbon deletion reaction of aryl azides to achieve a C → N atom transmutation.[32] In 2023, Levin et al. reported a similar, *ipso*-selective C → N atom transmutation.[33]

Received: October 16, 2023
Revised: January 8, 2024
Accepted: January 9, 2024
Published: January 29, 2024

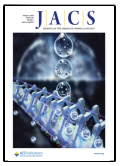

https://doi.org/10.1021/jacs.3c11515
J. Am. Chem. Soc. 2024, 146, 2950−2958

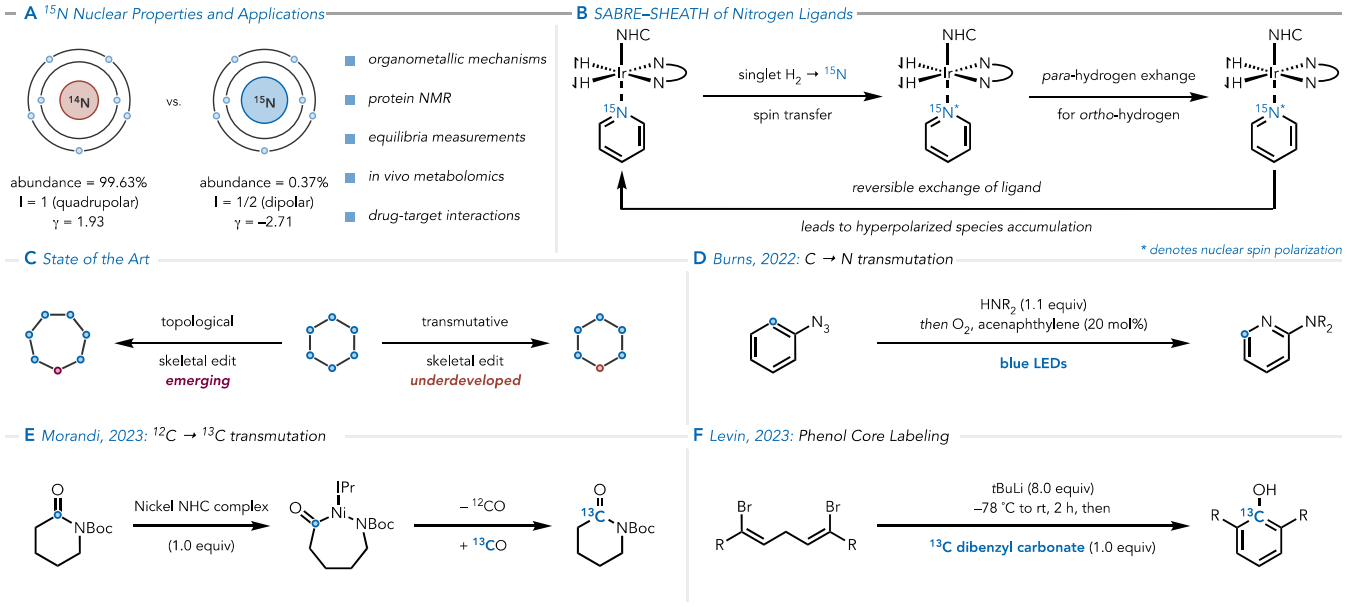

Figure 1. Motivation and background. (a) Nuclear properties and applications of ^{15}N. (b) Summary of the SABRE-SHEATH process for ^{15}N hyperpolarization in organometallic ligands. (c) Conceptual outline delineating topological and transmutative skeletal edits. (d) Summary of Burns et al.'s recent benzene-to-pyridine skeletal edit. (e) Summary of Morandi et al.'s recent skeletal metalation, which could be used to achieve an isotopic skeletal edit. (f) Summary of Levin et al.'s recent phenol core-labeling strategy.

In 2023, Morandi et al. published a method that enabled skeletal metalation of lactams, facilitating a $^{12}C \rightarrow {}^{13}C$ isotopic skeletal edit.[34] Interest has continued to grow in the paradigm of isotopic labeling of the skeletons of molecules. For example, in 2023, Levin et al. disclosed a facile synthesis of ^{13}C core-labeled phenols (Figure 1F) from a precursor *bis*-vinyl dibromide.[35]

Herein, we report a method using a modification of the established Zincke reaction that accomplishes a direct $^{14}N \rightarrow {}^{15}N$ atom swap in a wide variety of nitrogen heteroaromatics using an accessible, easy to prepare ^{15}N-enriched aspartate-derived diester. Key to this transformation is a low-temperature triflylation of the heterocyclic nitrogen atom, which permits a room-temperature Zincke-type ring-opening/ring-closure sequence mediated by an aspartate nucleophile to yield an isolable *N*-succinyl intermediate where the nitrogen in the ring has been swapped. Elimination of the succinyl group as fumarate or maleate *in situ* unveils the isotopically labeled heterocycle. Importantly, this transformation takes place rapidly under mild conditions on a diverse library of heteroaromatics in excellent chemical yields with generally useful levels of isotopic enrichment. This method directly enriches nitrogen heteroaromatics in complex molecules with ^{15}N using a readily available ^{15}N source enabling high-sensitivity, rapid magnetic resonance experimentation in a broader area of chemical space to impact drug development, materials science, molecular imaging, and molecular biology.

RESULTS AND DISCUSSION

Leveraging our prior work on a formal carbon atom deletion to convert pyrimidines to pyrazoles (Figure 2A),[36] we hypothesized that *N*-triflylated pyrimidine heterocycles would undergo an addition of nucleophile, ring opening, and ring closure[37] sequence to achieve a formal nitrogen deletion to yield **3** when exposed to an aminomalonate nucleophile (Figure 2B). Instead, exposing the *N*-triflylated heterocycle to the aminomalonate led to *N*-malonyl ylide **4**, which was confirmed by X-ray crystallographic analysis. Because this conversion accomplished a nitrogen-to-nitrogen atom swap in accordance with established Zincke transamination, we recognized the potential utility of this transformation if ^{15}N-isotopically labeled nucleophiles were employed. With this application in mind, we sought to optimize for the formation of the *N*-malonyl pyrimidinium ylide, where a nitrogen in the skeleton of the heteroaromatic had been exchanged (see the Supporting Information for details). However, the variable protonation state of the malonyl ylide (methine C–H $pK_a \approx 5.0$)[38] and competing side reactions such as *bis*-addition of the amine nucleophile to the activated heterocycle (giving **15**, Figure 2D) led to variable yields. Additionally, removal of the malonyl group from the ylide intermediate proved to be challenging and similarly irreproducible. We hypothesized that these issues arose from the high C–H acidity of the malonyl fragment; therefore, we evaluated an aspartate diester in lieu of an aminomalonate (Figure 2C), which led to higher, reproducible reaction yields of up to 99%. This nucleophile also set the stage for dealkylation of the *N*-alkyl intermediate—which is precedented for the analogous pyridine system[39]—to give a pyrimidine ring in which one of the nitrogen atoms had been exchanged.

Mechanistically, as shown in Figure 2D, aminomalonate and aspartate nucleophiles are presumed to attack *N*-triflylpyrimidinium species **9** at C6 as in the Zincke ANRORC sequence,[23,37] analogous to our previously reported observations with hydrazine in the pyrimidine-to-pyrazole transformation (Figure 2A). Dearomatized adduct **10** could undergo a related 6π electrocyclic ring opening, leading to *aza*-Zincke imine intermediate **11**.[23,24,40] Since the aspartate nitrogen atom that initially attacked the pyrimidinium remains the most nucleophilic atom in the molecule, this nitrogen attacks at C2 (favoring a 6-*exo-trig* over a 4-*exo-trig* cyclization) resulting in ring-closed *N*-succinyl dihydro-aminopyrimidine intermediate **12**. Rearomatization by elimination of triflamide

https://doi.org/10.1021/jacs.3c11515
J. Am. Chem. Soc. 2024, 146, 2950–2958

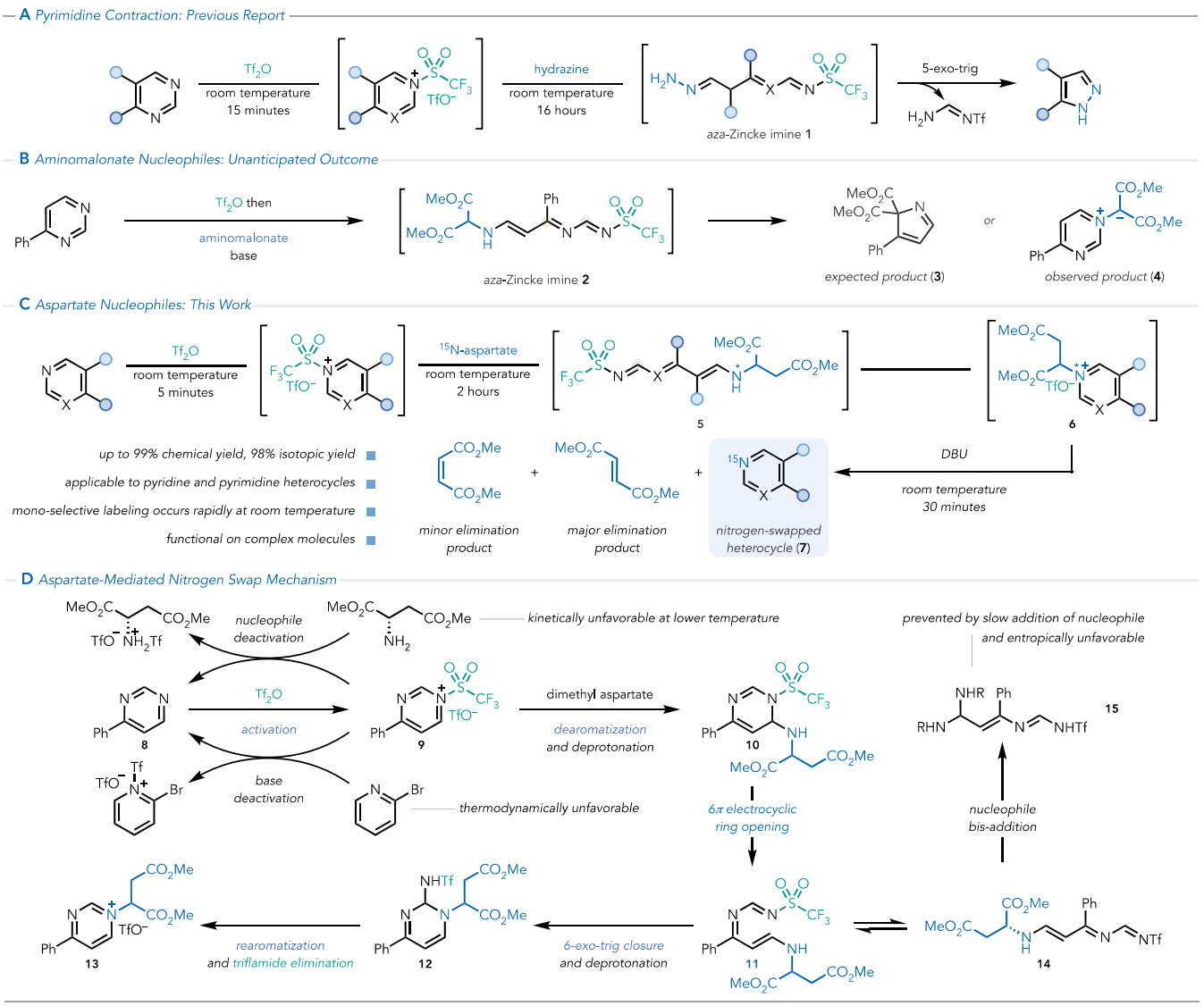

Figure 2. Background and introduction to the present disclosure. (a) Summary of our prior work on the triflylation-promoted ring contraction of pyrimidines by formal carbon deletion. (b) Unexpected formation of *N*-malonyl pyrimidinium ylides when triflylated pyrimidines were exposed to aminomalonate nucleophiles. (c) Adjusted conditions using aspartate nucleophiles to generate *N*-succinyl pyrimidinium or pyridinium salts and summary of the present report. (d) Proposed mechanism for the formation of *N*-succinyl pyrimidinium triflate salts.

gives **13** followed by addition of DBU to facilitate elimination of the succinyl group yielding the neutral heteroaromatic, where the highlighted nitrogen has been exchanged (**7**, Figure 2C).

Optimization data for this reaction are shown in Table 1. Elimination of the succinyl fragment occurs readily at room temperature upon the addition of DBU (optimally as a solution in DCM) to the *N*-succinyl species. Using these optimized conditions, we proceeded to evaluate the scope of this reaction on a small library of pyrimidine-containing compounds. These results are summarized in Figure 3. Some substrates exhibited major and minor sites of ^{15}N incorporation, as observed by ^{15}N NMR; the positions exhibiting the higher ^{15}N enrichment are depicted. The positional selectivity of ^{15}N labeling is influenced by sterics; greater labeling occurs at the less hindered pyrimidine nitrogen, corresponding to the attack of the aspartate nucleophile at the least hindered carbon. Simple 4-arylpyrimidines **18**–**24** were found to undergo ^{15}N labeling in high chemical and isotopic yields (Figure 3A).

Table 1. Effect of the Solvent and Base for Aspartate-Mediated Transamination in Pyrimidines

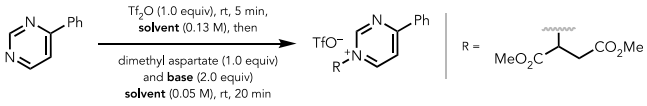

entry	solvent	base	yield (%)[a]
1	dichloroethane	2-chloropyridine	85
2	chloroform	2-chloropyridine	89
3	dichloromethane	2-chloropyridine	82
4	dioxane	2-chloropyridine	83
5	dichloroethane	2,6-lutidine	65
6	dichloroethane	dtbpy	58
7	dichloroethane	2-bromopyridine	96
8	**dichloroethane**	**2-bromopyridine**	**99**[b]

[a]Determined by ^{1}H NMR using 1,3,5-trimethoxybenzene as an internal standard. [b]1.2 equiv of triflic anhydride and 1.5 equiv of dimethyl aspartate.

https://doi.org/10.1021/jacs.3c11515
J. Am. Chem. Soc. 2024, 146, 2950−2958

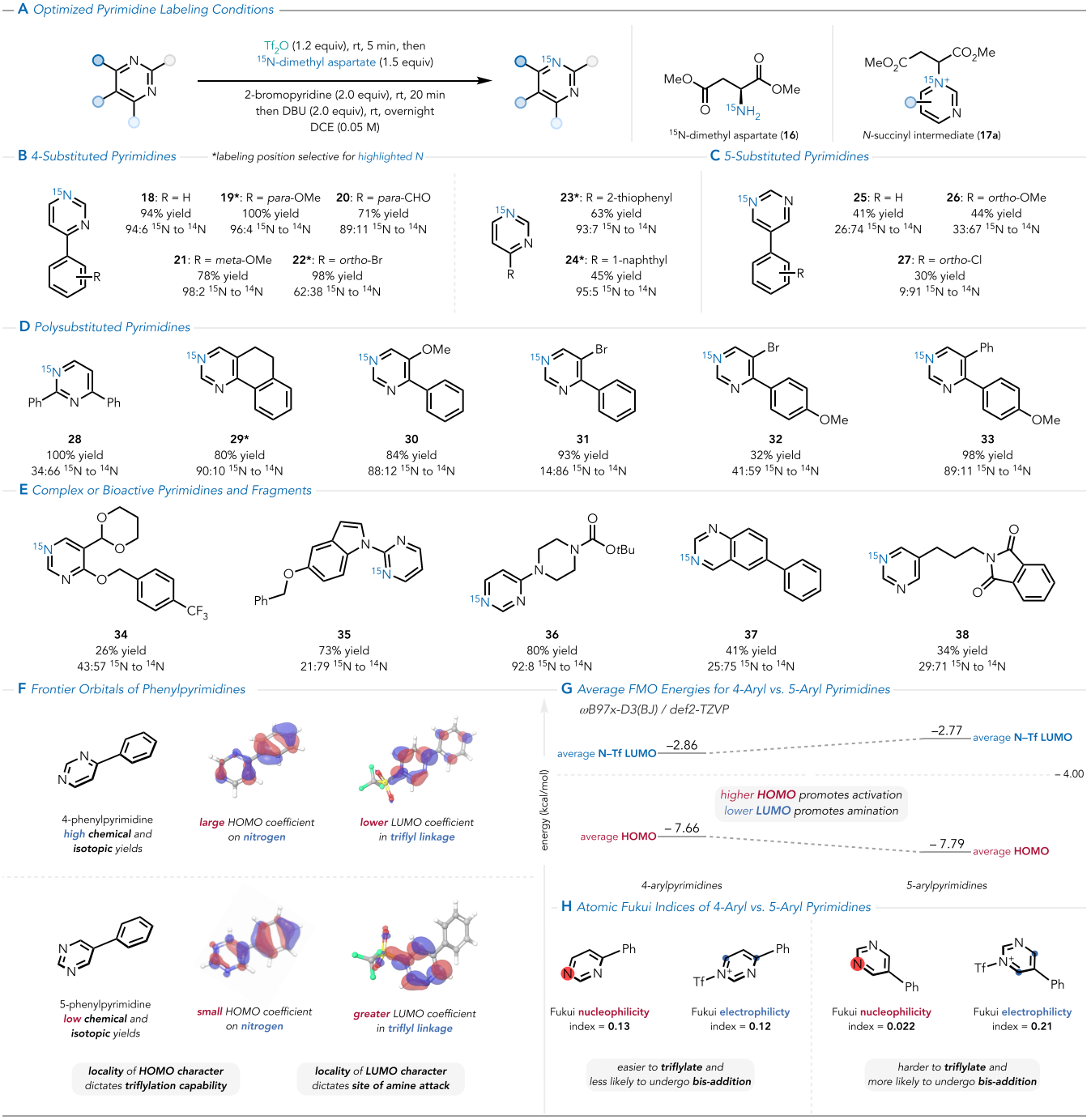

Figure 3. Performance of pyrimidine-containing substrates in isotopic exchange reaction. (a) Optimized conditions for the $^{14}N \rightarrow {}^{15}N$ isotopic skeletal edit of pyrimidines. (b) Summary of 4-aryl and 4-heteroaryl pyrimidine substrates. (c) Summary of 5-aryl pyrimidine substrates. (d) Summary of disubstituted pyrimidine substrates. (e) Summary of complex substrates. (f) Frontier molecular orbitals for 4-phenylpyrimidine and 5-phenylpyrimidine. (g) Average frontier molecular orbital energies for 4-aryl vs 5-aryl pyrimidines. (h) Fukui indices for 4-aryl vs 5-aryl pyrimidines.

Other arenes were also tolerated at C4 (see **23** and **24**). 5-Arylpyrimidines **25**–**27** also underwent labeling (Figure 3B), albeit with a lower efficiency. This discrepancy is likely due to the lower electron density (and thus nucleophilicity) of the participating pyrimidine nitrogen in the 5-aryl substrates relative to the 4-aryl substrates. Pyrimidines bearing electron-poor arenes do not undergo appreciable amounts of labeling, supporting this hypothesis. The successful participation of 4,5-diaryl pyrimidine **33** implies that electronics at nitrogen dictate the success of the reaction to a greater degree than the steric encumbrance about the heterocyclic carbon atoms. We posit that 4-aryl pyrimidines undergo triflylation to a greater degree and feature a stronger N–S bond, rendering the activated species more resistant to detriflylation to give an unlabeled starting material. The low chemical yields for the 5-arylpyrimidines likely resulted from decomposition under the reaction conditions, possibly due to *bis*-addition of the aspartate nucleophile to the pyrimidine heterocycle (as determined by mass spectrometry) and subsequent side

https://doi.org/10.1021/jacs.3c11515
J. Am. Chem. Soc. 2024, 146, 2950–2958

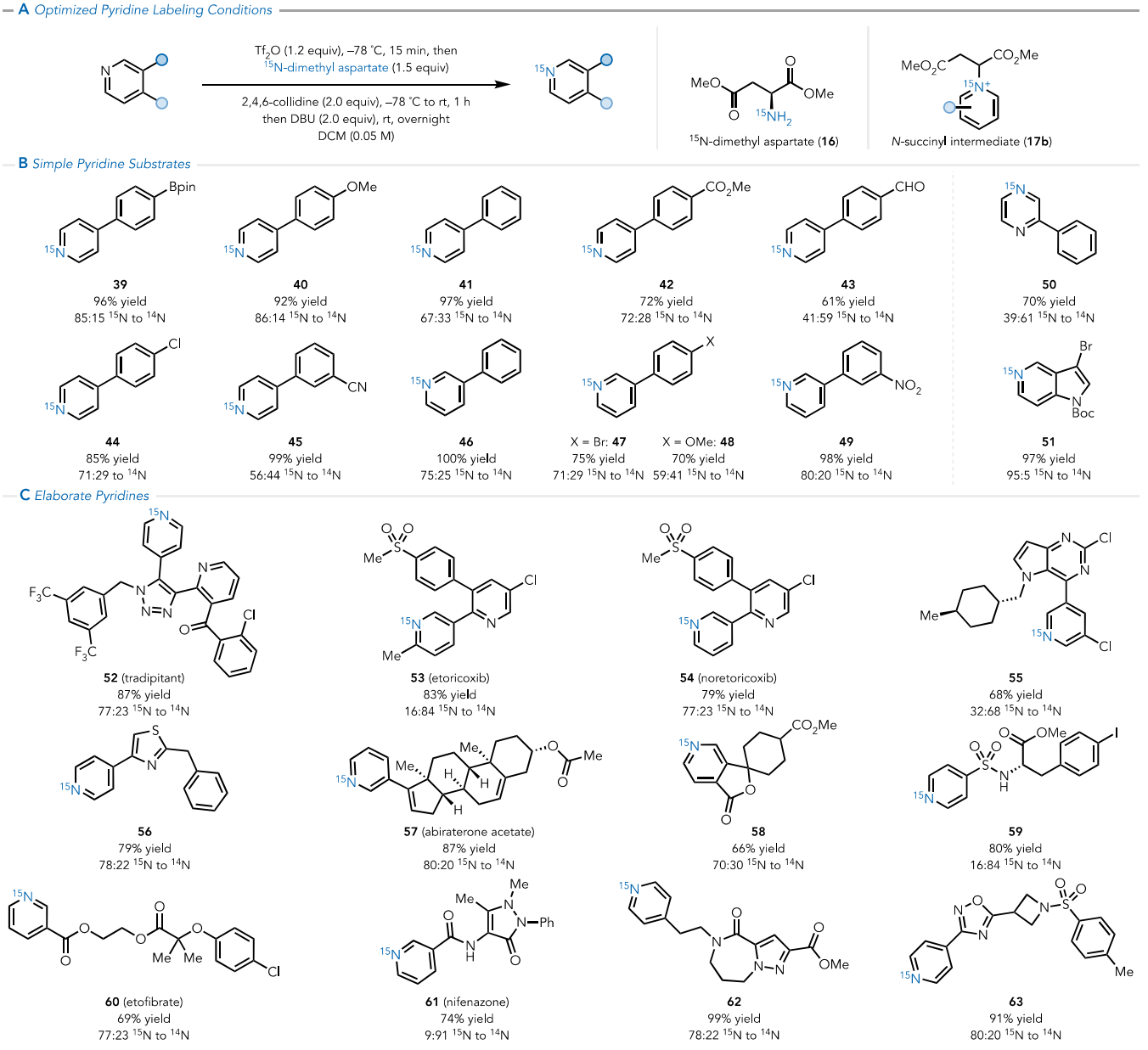

Figure 4. Performance of pyridine-containing substrates in isotopic exchange reaction. (a) Optimized conditions for the $^{14}N \rightarrow {}^{15}N$ isotopic skeletal edit of pyridines. (b) Summary of 3-aryl and 4-arylpyridine substrates. (c) Summary of elaborate or bioactive pyridine substrates.

reactions of the *bis*-adduct. These hypotheses are supported by our computational studies (Figure 3F,G, *vide infra*).

Polysubstituted pyrimidines also participated in the $^{14}N \rightarrow {}^{15}N$ exchange as summarized in Figure 3D. Importantly, 2-substituted pyrimidines **28** and **35** were found to undergo ^{15}N labeling in serviceable yields (see the Supporting Information for details). For 2-substituted pyrimidines, there is a large steric barrier associated with the triflylation step, which correspondingly renders the triflyl motif more susceptible to attack by a nucleophile in the resulting pyrimidinium species. These factors likely explain the lower labeling yields observed for 2-substituted substrates. C5-functionalized pyrimidines **30**–**32** also participated in the reaction, with higher chemical and isotopic yields observed for electron-rich pyrimidines. Finally, several elaborated pyrimidines underwent labeling with variable degrees of success (Figure 3E). Practically, the yields of several "complex" pyrimidines were limited by poor solubility in the reaction medium. Additionally, the inherently low nucleophilicity of the pyrimidine heterocycle often led to competing triflylation at other more reactive sites on these molecules, preventing the desired reaction or inducing side reactivity. Relative to the C5-aryl-substituted pyrimidines, on average, the 4-arylpyrimidine substrates feature larger HOMO coefficients on the heterocyclic nitrogen atoms and higher-lying HOMOs, indicative of enhanced nucleophilicity. In fact, the HOMOs of the 5-arylpyrimidine substrate are minimally localized on heterocyclic nitrogen atoms (Figure 3F). The *N*-triflyl derivatives of the 5-arylpyrimidines also feature greater LUMO character on the heterocyclic carbon atoms and are less sterically hindered at these sites, indicating a higher likelihood of deleterious *bis*-nucleophile addition (Figure 3G). These data are corroborated by the Fukui nucleophilicity and electro-

https://doi.org/10.1021/jacs.3c11515
J. Am. Chem. Soc. 2024, 146, 2950–2958

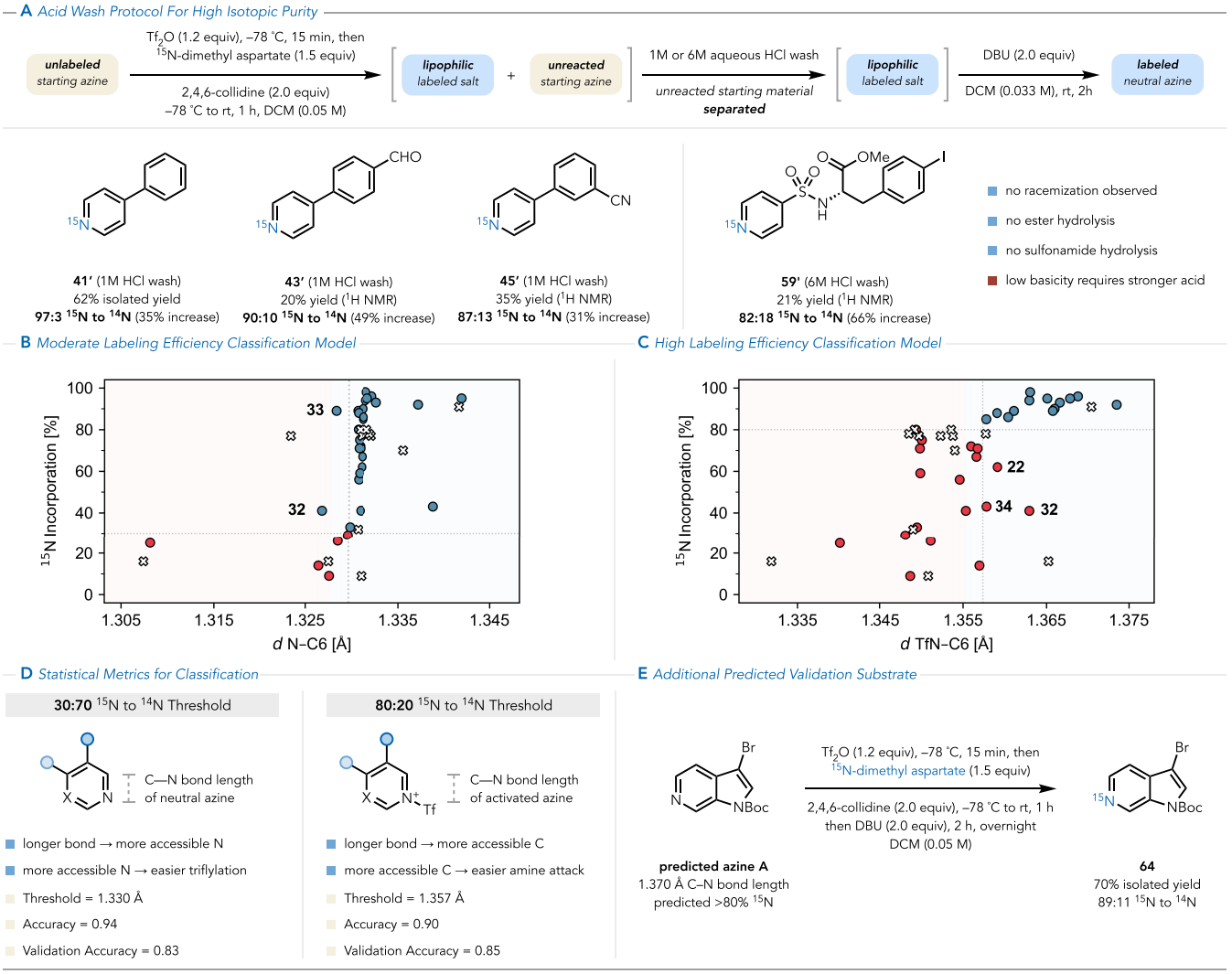

Figure 5. (a) Acid wash protocol for increasing isotopic yield by removing the unreacted starting material from the chemically distinct, labeled *N*-succinyl species. (b,c) Classification models categorizing substrates based on ^{15}N incorporation—(b) below or above 30% and (c) below or above 80%. Red and blue circles represent substrates below or above the respective threshold line. Substrates used for validation are marked with crosses. (d) Statistical data for classification models. (e) Additional substrate for forward prediction validation.

philicity indices for the nitrogen and carbon atoms of the neutral and triflylated species, respectively (Figure 3H).

We then hypothesized that these reaction conditions should achieve an analogous transformation of pyridines. Indeed, we have found that an electronically diverse set of pyridines undergo labeling through the ANRORC sequence and the intermediacy of *N*-succinylpyridinium species. Optimization of this reaction on pyridine substrates (see the Supporting Information for details) led to the identification of conditions similar to those previously established by McNally and co-workers in 2022 for the ring opening of *N*-triflylpyridinium species for site-selective halogenation.[41] Though this reaction was successful at room temperature, performing the triflylation and amine addition at −78 °C significantly improved the yields (Figure 4A).

Pyridines **39**–**49** generally underwent $^{14}N \rightarrow {}^{15}N$ exchange when exposed to these modified conditions in moderate to high yield with a clear bias toward electron-rich (and therefore more nucleophilic) pyridines (Figure 4B). *para*-Aryl and *meta*-arylpyridines were well tolerated, though *ortho*-arylpyridines did not undergo ^{15}N labeling, likely due to steric congestion upon triflylation leading to a high barrier for the 6-*exo*-*trig* cyclization required for labeling. Accordingly, when 2,2′-bipyridine and pyriproxyfen (a 2-substituted bioactive pyridine) were subjected to the reaction conditions, the starting materials (i.e., the naturally abundant isotopologues) were recovered quantitatively. Pyrazine **50** and 6/5 fused pyridine **51** also participated, demonstrating the application of the protocol to analogous heterocycles.

Elaborated pyridines **52**–**63** were found to undergo labeling in moderate to high chemical and isotopic yields (Figure 4C). Since the pyridine nitrogen is more nucleophilic relative to the pyrimidine nitrogen atoms, competing reactive groups were better tolerated in these cases. In general, other aromatic heterocycles did not significantly impede the reaction. Importantly, several substrates bearing more than one pyridine (**52**, **53**, and **54**) underwent selective labeling on the more electron-rich, sterically accessible heterocycle. Small substituents at the 2-position on the pyridine ring were somewhat tolerated (e.g., **53**). However, the deleterious effect of 2-substitution is evident when comparing the isotopic yields of etoricoxib (**53**) and noretoricoxib (**54**), where the absence of

https://doi.org/10.1021/jacs.3c11515
J. Am. Chem. Soc. 2024, 146, 2950−2958

the 2-methyl substituent leads to a fivefold improvement in isotopic labeling. Some 2-substituted pyridines were found to undergo the transamination sequence when triflylated and exposed to β-alanine esters, likely due to the lower steric hindrance around the amine nitrogen atom relative to the branched aspartate nucleophile. The *N*-acrylylpyridinium salt formed in this way could undergo a similar DBU-mediated dealkylation by elimination of acrylate; however, because of the extremely limited availability of ^{15}N-β-alanine and marked instability of the free base amine under ambient conditions, this approach was not considered beyond preliminary investigations. Even electron-deficient pyridines (such as 3-chloropyridine **55** and 4-sulfonamidopyridine **59**) participated in the reaction. Enolizable phenylalanine derivative **59** did not undergo racemization (as confirmed by chiral HPLC analysis). Solubility challenges in dichloromethane at −78 °C were addressed by adding protective groups to some drug-like substrates (e.g., acetylation of abiraterone to the prodrug **57**);[42] this approach, however, was not applicable to nifenazone (**61**).

The use of a mild acid wash to remove unreacted starting material after transamination results in the isolation of the labeled pyridine product with a high isotopic purity. This sequence is summarized in Figure 5A. The isotopic distribution for the labeled product obtained by this method matched that of the labeled dimethyl aspartate nucleophile for the model substrate (4-phenylpyridine, **41′**). For substrates **43′**, **45′**, and **59′**, greatly enhanced isotopic distributions were achieved using this protocol as shown in Figure 5A.

To elucidate the structural features required to achieve either moderate (30:70 ^{15}N to ^{14}N) or high (80:20 ^{15}N to ^{14}N) isotopic ratios in the labeled products of this reaction (Figure 5C,D), we computed DFT descriptors for both the neutral starting materials and the corresponding triflylated intermediates. These thresholds were selected since 30% ^{15}N labeling is adequate for several practical applications, while achieving 80% labeling demonstrates the efficiency of the reaction. We subjected the entire set of pyrimidines and simple pyridines (in Figures 3 and 4) to single-node decision trees with the exception of the only examples of 2-substituted pyrimidines (i.e., **28** and **35**; see computational and modeling details in the Supporting Information).[43] We validated the models using the set of complex pyridine substrates depicted in Figure 4C, since these substrates represent medicinally relevant, complex examples. Using the 30% ^{15}N incorporation threshold (Figure 5A), the classification algorithm shows that substrates can be effectively binned according to the computed N−C6 distance in the parent compound (prior to triflylation) with 94% accuracy. Substrates with computed N−C6 bond distance > 1.330 Å consistently yield ^{15}N incorporation above 30%. This structural feature also suggests that as the N−C6 distance increases, the nitrogen atom becomes more nucleophilic and thus undergoes triflylation more effectively. Additionally, a longer N−C6 bond could also indicate reduced steric hindrance at nitrogen, further facilitating triflylation.

The model misclassified two pyrimidines (**32** and **33**), both of which possess a *para*-methoxyphenyl group at C4. As mentioned before, these compounds may form stronger N−S bonds, rendering them more resistant to detriflylation and increasing the observed isotopic yield relative to what is expected from the model. Finally, we validated the model's ability to predict isotopic yields using the complex pyridine set. Notably, none of the simple pyridines in the training set yielded ^{15}N incorporation below 30%, which led us to anticipate that testing the model's performance against pyridines with varied substitution, with their diverse isotopic yield range, could serve as a robustness test for the model. The validation test resulted in an 83% accuracy, demonstrating the potential applicability of this model.

The second classification model utilized an 80% ^{15}N incorporation threshold (Figure 5B), wherein the computed N−C6 bond length in the triflylated heterocycle serves as an effective criterion for categorizing substrates into those yielding high (>80%) or lower isotopic yield, achieving an accuracy of 90%. Triflylated substrates with computed N−C6 bond distances exceeding 1.357 Å consistently exhibit ^{15}N incorporation above 80%. Specifically, the model suggests that as the triflyl N−C6 bond length increases, C6 becomes more electrophilic, rendering this carbon atom more susceptible to nucleophilic attack. The model misclassified compounds **22**, **32**, and **34**, predicting isotopic labeling efficiency higher than what is empirically achieved. The simple model fails to account for additional reaction intricacies (e.g., increased reaction barrier for the 6π electrocyclic ring opening or the 6-*exo*-*trig* closure steps), which could potentially explain the observed misclassifications. Nonetheless, this model can be a valuable tool for anticipating substrates that can produce high isotopic yields. The model accuracy in the validation set is 85%, demonstrating robustness.

CONCLUSIONS

In summary, we have developed a one-step procedure to achieve single-atom isotopic transmutation from ^{14}N → ^{15}N in various heteroaromatics. This transformation proceeds through the intermediacy of the corresponding *N*-triflylated heterocycle, followed by a ^{15}N-aspartate diester-mediated ANRORC process and subsequent succinyl elimination to give the isotopically enriched product. High chemical yields and moderate to high isotopic ratios are typically observed, even for complex or drug-like molecules. Two classification models were implemented to assess isotopic labeling efficiency using stereoelectronic parameters; both indicated that longer N−C6 bond distances in the neutral or triflylated substrates were associated with enhanced labeling efficiency. Notably, products possessing isotopic enrichment matching that of the labeled dimethyl aspartate can be isolated through a slightly modified procedure, which is valuable for applications requiring high isotopic purity. As nitrogen-containing heterocycles are prevalent in complex functional molecules, such as pharmaceuticals, we envision that the isotopic enrichment of these molecules without resorting to lengthy *de novo* syntheses will enable studies in mechanism elucidation, *in vivo* metabolomics, spin hyperpolarization, and more.

ASSOCIATED CONTENT

Supporting Information

The Supporting Information is available free of charge at https://pubs.acs.org/doi/10.1021/jacs.3c11515.

Experimental procedures, characterization data, spectra for all new compounds, crystallographic data, and computational details (PDF)

Cartesian coordinates of DFT-optimized structures (PDF)

Calculated molecular and atomic parameters (XLSX)

https://doi.org/10.1021/jacs.3c11515
J. Am. Chem. Soc. 2024, 146, 2950−2958

Accession Codes

CCDC 2296598 and 2299080 contain the supplementary crystallographic data for this paper. These data can be obtained free of charge via www.ccdc.cam.ac.uk/data_request/cif, or by emailing data_request@ccdc.cam.ac.uk, or by contacting The Cambridge Crystallographic Data Centre, 12 Union Road, Cambridge CB2 1EZ, UK; fax: +44 1223 336033.

AUTHOR INFORMATION

Corresponding Authors

Matthew S. Sigman − *Department of Chemistry, University of Utah, Salt Lake City, Utah 84112, United States;* orcid.org/0000-0002-5746-8830; Email: matt.sigman@utah.edu

Charles S. Yeung − *Discovery Chemistry, Merck & Co., Inc., Boston, Massachusetts 02115, United States;* orcid.org/0000-0001-7320-7190; Email: charles.yeung@merck.com

Richmond Sarpong − *Department of Chemistry, University of California, Berkeley, Berkeley, California 94720, United States;* orcid.org/0000-0002-0028-6323; Email: rsarpong@berkeley.edu

Authors

G. Logan Bartholomew − *Department of Chemistry, University of California, Berkeley, Berkeley, California 94720, United States;* orcid.org/0000-0002-3023-4460

Samantha L. Kraus − *Department of Chemistry, University of California, Berkeley, Berkeley, California 94720, United States*

Lucas J. Karas − *Department of Chemistry, University of Utah, Salt Lake City, Utah 84112, United States*

Filippo Carpaneto − *Department of Chemistry, University of California, Berkeley, Berkeley, California 94720, United States;* Present Address: Department of Chemistry, University of Chicago, Chicago, Illinois 60637, United States

Raffeal Bennett − *Discovery Analytical Research, Merck & Co., Inc., Boston, Massachusetts 02115, United States;* orcid.org/0000-0002-0628-0774

Complete contact information is available at: https://pubs.acs.org/10.1021/jacs.3c11515

Author Contributions

The manuscript was written through contributions of all authors.

Funding

R.S. is grateful to the National Institute of General Medical Sciences (NIGMS R35 GM130345), Merck Sharp & Dohme LLC, a subsidiary of Merck & Co., Inc., Rahway, NJ, USA (MSD), and the National Science Foundation (NSF) under the Center for Computer-Assisted Synthesis (CCAS) for financial support (NSF CHE 2202693). G.L.B. (NSF 2021294420) and S.L.K. (NSF 2022331906) thank the National Science Foundation for graduate fellowships. Instruments in CoC-NMR are supported in part by National Institutes of Health (NIH S10OD024998). The CoC-MGCF was supported in part by NIH S10OD023532.

Notes

The authors declare the following competing financial interest(s): R.S. is a paid consultant for Merck Sharp & Dohme LLC, a subsidiary of Merck & Co., Inc., Rahway, NJ, USA. The authors declare no other competing interests.

ACKNOWLEDGMENTS

We acknowledge the help and support of the following people from MSD: S. Burgess for assistance in NMR structure elucidation; L. M. Nogle, D. A. Smith, A. Beard, M. Darlak, and M. Pietrafitta for reversed-phase purifications; and M. Lux and H. Park for a thorough review of the manuscript and helpful discussions. We thank Dr. Hasan Celik and UC Berkeley's NMR facility in the College of Chemistry (CoC-NMR) for spectroscopic assistance. We thank Dr. Nicholas Settineri (UC Berkeley) for X-ray crystallographic studies of **4** and **S26**. We are grateful to Dr. Kathy Durkin and Dr. Dave Small for computational guidance. We thank Zhongrui Zhou and Ulla Anderson in the QB3/Department of Chemistry Mass Spectrometry Facility for accurate mass measurements. The support and resources from the Center for High Performance Computing at the University of Utah are gratefully acknowledged.

REFERENCES

(1) Nelissen, F. H. T.; Tessari, M.; Wijmenga, S. S.; Heus, H. A. Stable Isotope Labeling Methods for DNA. *Prog. Nucl. Magn. Reson. Spectrosc.* **2016**, *96*, 89−108.

(2) Gevaert, K.; Impens, F.; Ghesquière, B.; Van Damme, P.; Lambrechts, A.; Vandekerckhove, J. Stable Isotopic Labeling in Proteomics. *Proteomics* **2008**, *8*, 4873−4885.

(3) Von Philipsborn, W.; Müller, R. ^{15}N-NMR Spectroscopy—New Methods and Applications [New Analytical Methods (28)]. *Angew. Chem., Int. Ed. Engl.* **1986**, *25*, 383−413.

(4) *Protein NMR Spectroscopy: Principles and Practice*; Cavanagh, J., Ed.; Academic Press: San Diego, 1996.

(5) Nowakowski, M.; Saxena, S.; Stanek, J.; Żerko, S.; Koźmiński, W. Applications of High Dimensionality Experiments to Biomolecular NMR. *Prog. Nucl. Magn. Reson. Spectrosc.* **2015**, *90*−*91*, 49−73.

(6) Vitaku, E.; Smith, D. T.; Njardarson, J. T. Analysis of the Structural Diversity, Substitution Patterns, and Frequency of Nitrogen Heterocycles among U.S. FDA Approved Pharmaceuticals: Miniperspective. *J. Med. Chem.* **2014**, *57*, 10257−10274.

(7) Shearer, J.; Castro, J. L.; Lawson, A. D. G.; MacCoss, M.; Taylor, R. D. Rings in Clinical Trials and Drugs: Present and Future. *J. Med. Chem.* **2022**, *65*, 8699−8712.

(8) Campos, K. R.; Coleman, P. J.; Alvarez, J. C.; Dreher, S. D.; Garbaccio, R. M.; Terrett, N. K.; Tillyer, R. D.; Truppo, M. D.; Parmee, E. R. The Importance of Synthetic Chemistry in the Pharmaceutical Industry. *Science* **2019**, *363*, No. eaat0805.

(9) Marek, R.; Lycka, A. ^{15}N NMR Spectroscopy in Structural Analysis. *COC* **2002**, *6*, 35−66.

(10) May, D. S.; Crnkovic, C. M.; Krunic, A.; Wilson, T. A.; Fuchs, J. R.; Orjala, J. E. ^{15}N Stable Isotope Labeling and Comparative Metabolomics Facilitates Genome Mining in Cultured Cyanobacteria. *ACS Chem. Biol.* **2020**, *15*, 758−765.

(11) Ramirez, B.; Durst, M. A.; Lavie, A.; Caffrey, M. NMR-Based Metabolite Studies with ^{15}N Amino Acids. *Sci. Rep.* **2019**, *9*, 12798.

(12) Nakabayashi, R.; Mori, T.; Takeda, N.; Toyooka, K.; Sudo, H.; Tsugawa, H.; Saito, K. Metabolomics with ^{15}N Labeling for Characterizing Missing Monoterpene Indole Alkaloids in Plants. *Anal. Chem.* **2020**, *92*, 5670−5675.

(13) Blasco, T. Insights into Reaction Mechanisms in Heterogeneous Catalysis Revealed by in Situ NMR Spectroscopy. *Chem. Soc. Rev.* **2010**, *39*, 4685.

(14) Shestakova, T. S.; Shenkarev, Z. O.; Deev, S. L.; Chupakhin, O. N.; Khalymbadzha, I. A.; Rusinov, V. L.; Arseniev, A. S. Long-Range ^{1}H-^{15} N *J* Couplings Providing a Method for Direct Studies of the Structure and Azide-Tetrazole Equilibrium in a Series of Azido-1,2,4-Triazines and Azidopyrimidines. *J. Org. Chem.* **2013**, *78*, 6975−6982.

(15) Cheatham, S.; Gierth, P.; Bermel, W.; Kupče, Ē. HCNMBC - A Pulse Sequence for H-(C)-N Multiple Bond Correlations at Natural Isotopic Abundance. *J. Magn. Reson.* **2014**, *247*, 38−41.

(16) Cheatham, S.; Kline, M.; Kupče, E. Exploiting Natural Abundance ^{13}C-^{15}N Coupling as a Method for Identification of Nitrogen Heterocycles: Practical Use of the HCNMBC Sequence: Practical Use of the HCNMBC Sequence. *Magn. Reson. Chem.* **2015**, *53*, 363−368.
(17) Deev, S. L.; Shestakova, T. S.; Charushin, V. N.; Chupakhin, O. N. Synthesis and Azido-Tetrazole Tautomerism of 3-Azido-1,2,4-Triazines. *Chem. Heterocycl. Compd.* **2017**, *53*, 963−975.
(18) Deev, S. L.; Khalymbadzha, I. A.; Shestakova, T. S.; Charushin, V. N.; Chupakhin, O. N. ^{15}N Labeling and Analysis of ^{13}C-^{15}N and ^{1}H-^{15}N Couplings in Studies of the Structures and Chemical Transformations of Nitrogen Heterocycles. *RSC Adv.* **2019**, *9*, 26856−26879.
(19) Truong, M. L.; Theis, T.; Coffey, A. M.; Shchepin, R. V.; Waddell, K. W.; Shi, F.; Goodson, B. M.; Warren, W. S.; Chekmenev, E. Y. ^{15}N Hyperpolarization by Reversible Exchange Using SABRE-SHEATH. *J. Phys. Chem. C* **2015**, *119*, 8786−8797.
(20) Shchepin, R. V.; Barskiy, D. A.; Coffey, A. M.; Theis, T.; Shi, F.; Warren, W. S.; Goodson, B. M.; Chekmenev, E. Y. ^{15}N Hyperpolarization of Imidazole-$^{15}N_2$ for Magnetic Resonance pH Sensing via SABRE-SHEATH. *ACS Sens.* **2016**, *1*, 640−644.
(21) Kovtunov, K. V.; Kovtunova, L. M.; Gemeinhardt, M. E.; Bukhtiyarov, A. V.; Gesiorski, J.; Bukhtiyarov, V. I.; Chekmenev, E. Y.; Koptyug, I. V.; Goodson, B. M. Heterogeneous Microtesla SABRE Enhancement of ^{15}N NMR Signals. *Angew. Chem.* **2017**, *129*, 10569−10573.
(22) Shchepin, R. V.; Barskiy, D. A.; Mikhaylov, D. M.; Chekmenev, E. Y. Efficient Synthesis of Nicotinamide-1-^{15}N for Ultrafast NMR Hyperpolarization Using Parahydrogen. *Bioconjugate Chem.* **2016**, *27*, 878−882.
(23) Cheng, W.-C.; Kurth, M. J. The Zincke Reaction: A Review. *Org. Prep. Proced. Int.* **2002**, *34*, 585−608.
(24) Vanderwal, C. D. Reactivity and Synthesis Inspired by the Zincke Ring-Opening of Pyridines. *J. Org. Chem.* **2011**, *76*, 9555−9567.
(25) Phan, A. T.; Patel, D. J. A Site-Specific Low-Enrichment ^{15}N, ^{13}C Isotope-Labeling Approach to Unambiguous NMR Spectral Assignments in Nucleic Acids. *J. Am. Chem. Soc.* **2002**, *124*, 1160−1161.
(26) Pomin, V. H.; Sharp, J. S.; Li, X.; Wang, L.; Prestegard, J. H. Characterization of Glycosaminoglycans by ^{15}N NMR Spectroscopy and *in vivo* Isotopic Labeling. *Anal. Chem.* **2010**, *82*, 4078−4088.
(27) Andriukonis, E.; Gorokhova, E. Kinetic ^{15}N-Isotope Effects on Algal Growth. *Sci. Rep.* **2017**, *7*, 44181.
(28) He, J.; Zhang, X.; He, Q.; Guo, H.; Fan, R. Synthesis of ^{15}N-Labeled Heterocycles *via* the Cleavage of C-N Bonds of Anilines and Glycine-^{15}N. *Chem. Commun.* **2021**, *57*, 5442−5445.
(29) Chukanov, N. V.; Shchepin, R. V.; Joshi, S. M.; Kabir, M. S. H.; Salnikov, O. G.; Svyatova, A.; Koptyug, I. V.; Gelovani, J. G.; Chekmenev, E. Y. Synthetic Approaches for ^{15}N-Labeled Hyperpolarized Heterocyclic Molecular Imaging Agents for ^{15}N NMR Signal Amplification by Reversible Exchange in Microtesla Magnetic Fields. *Chem.—Eur. J.* **2021**, *27*, 9727−9736.
(30) Oppenheimer, N. J.; Matsunaga, T. O.; Kam, B. L. Synthesis of ^{15}N Nicotinamide: A General, One Step Synthesis of ^{15}N Labeled Pyridine Heterocycles. *J. Labelled Compd. Radiopharm.* **1978**, *15*, 191−196.
(31) Jurczyk, J.; Woo, J.; Kim, S. F.; Dherange, B. D.; Sarpong, R.; Levin, M. D. Single-Atom Logic for Heterocycle Editing. *Nat. Synth.* **2022**, *1*, 352−364.
(32) Patel, S. C.; Burns, N. Z. Conversion of Aryl Azides to Aminopyridines. *J. Am. Chem. Soc.* **2022**, *144*, 17797−17802.
(33) Pearson, T. J.; Shimazumi, R.; Driscoll, J. L.; Dherange, B. D.; Park, D.-I.; Levin, M. D. Aromatic Nitrogen Scanning by *Ipso*-Selective Nitrene Internalization. *Science* **2023**, *381*, 1474−1479.
(34) Zhong, H.; Egger, D. T.; Gasser, V. C. M.; Finkelstein, P.; Keim, L.; Seidel, M. Z.; Trapp, N.; Morandi, B. Skeletal Metalation of Lactams through a Carbonyl-to-Nickel-Exchange Logic. *Nat. Commun.* **2023**, *14*, 5273.
(35) Lynch, C. F.; Downey, J. W.; Zhang, Y.; Hooker, J. M.; Levin, M. D. Core-Labeling (Radio) Synthesis of Phenols. *Org. Lett.* **2023**, *25*, 7230−7235.
(36) Bartholomew, G. L.; Carpaneto, F.; Sarpong, R. Skeletal Editing of Pyrimidines to Pyrazoles by Formal Carbon Deletion. *J. Am. Chem. Soc.* **2022**, *144*, 22309−22315.
(37) Van Der Plas, H. C. The S_N(ANRORC) Mechanism: A New Mechanism for Nucleophilic Substitution. *Acc. Chem. Res.* **1978**, *11*, 462−468.
(38) Kobayashi, Y.; Kutsuma, T.; Morinaga, K.; Fujita, M.; Hanzawa, Y. Studies on the Reactions of Heterocyclic Compounds. IV. Preparations and Reactions of Heterocyclic *N*-Ylides. *Chem. Pharm. Bull.* **1970**, *18*, 2489−2498.
(39) Choi, J.; Laudadio, G.; Godineau, E.; Baran, P. S. Practical and Regioselective Synthesis of C-4-Alkylated Pyridines. *J. Am. Chem. Soc.* **2021**, *143*, 11927−11933.
(40) Toscano, R. A.; Hernandez-Galindo, M. D. C.; Rosas, R.; Garcia-Mellado, O.; Rio Portilla, F. D.; Amabile-Cuevas, C.; Alvarez-Toledano, C. Nucleophilic Reactions on 1-Trifluoromethanesulfonylpyridinium Trifluoromethanesulfonate (Triflylpyridinium Triflate, TPT). Ring-Opening and "Unexpected" 1,4-Dihydropyridine Reaction Products. *Chem. Pharm. Bull.* **1997**, *45*, 957−961.
(41) Boyle, B. T.; Levy, J. N.; De Lescure, L.; Paton, R. S.; McNally, A. Halogenation of the 3-Position of Pyridines through Zincke Imine Intermediates. *Science* **2022**, *378*, 773−779.
(42) Logothetis, C. J.; Efstathiou, E.; Manuguid, F.; Kirkpatrick, P. Abiraterone Acetate. *Nat. Rev. Drug Discovery* **2011**, *10*, 573−574.
(43) Newman-Stonebraker, S. H.; Smith, S. R.; Borowski, J. E.; Peters, E.; Gensch, T.; Johnson, H. C.; Sigman, M. S.; Doyle, A. G. Univariate Classification of Phosphine Ligation State and Reactivity in Cross-Coupling Catalysis. *Science* **2021**, *374*, 301−308.

NOTE ADDED IN PROOF

Several papers describing related transformations from the McNally (https://doi.org/10.1021/jacs.3c12445), Smith (https://doi.org/10.1021/jacs.3c11618), and Audisio (https://doi.org/10.26434/chemrxiv-2023-r0xn7) groups appeared in the literature since the initial submission of this work.

https://doi.org/10.1021/jacs.3c11515
J. Am. Chem. Soc. 2024, 146, 2950−2958